TBC

Includes five completely rewritten and updated fundamentals chapters and specialized chapters for six new industries – all by leading professionals in the field

Process objectives are critical to the successful manufacturing of a product. If the scale-up of mixing conditions fails to produce the required results, the costs of manufacturing can increase significantly. Although there are several industrial operations in which mixing requirements are readily scaled up from established correlations, many operations require a more thorough evaluation. *Advances in Industrial Mixing* provides practical insights from the leading professionals in the field and presents the latest methods for recognizing these more complex operations.

Advances in Industrial Mixing is a companion to the *Handbook of Industrial Mixing*. It reworks areas that have seen significant progress since the first edition and includes:

- Brand new chapters for 6 areas of industrial application: pharmaceutical validation, crystallization, water treatment, commissioning of mixing equipment, and safety
- Additional sections or examples for 5 chapters from the first edition including: magnetic drives, micromixers, vessel head volume calculations, additional information on heat transfer, and application of the Bourne protocol to reactor design
- Concise but critical technical updates for mixing in pipelines, turbulence, and CFD
- Five completely new fundamentals chapters covering: mean age distrbution, rheology and complex fluids, flow patterns, viscous mixing and solid-liquid mixing
- A full technical definition of mixing

The volume is a welcome addition to the *Handbook of Industrial Mixing* for the practicing engineer who needs to both identify and solve mixing problems

This book also provides concise discussions on theoretical background and uses many illustrative examples when covering applications. It includes a USB with a searchable pdf copy of the first edition, twenty tutorials on mixing, and a collection of video clips and animations of mixing processes, many of which are new for this edition.

SUZANNE M. KRESTA is a Professor in the Department of Chemical and Materials Engineering at the University of Alberta. She has worked with over 20 industries on various mixing problems.

ARTHUR WILLIAM ETCHELLS III is a retired DuPont Fellow with over forty years consulting in industrial mixing.

DAVID S. DICKEY is a consultant specializing in mixing processes and equipment with MixTech, Inc. He has more than forty years experience with mixing processes and equipment.

VICTOR ATIEMO-OBENG is retired from The Dow Chemical Company where he worked as a scientist in the Engineering Science and Market Development department.

THE NORTH AMERICAN MIXING FORUM provides an opportunity for dialogue about mixing problems in a wide range of industrial applications.

Cover Image: Courtesy of Coanda

ISBN 978-0-470-52382-7

9 780470 523827

www.wiley.com

WILEY

Also available
as an e-book

Kresta
Etchells III
Dickey
Atiemo-Obeng

Advances in Industrial Mixing

WILEY

DVD-ROM

Advances in Industrial Mixing

A Companion to the Handbook of Industrial Mixing

Edited by
Suzanne M. Kresta
Arthur W. Etchells III
David S. Dickey
Victor A. Atiemo-Obeng

Sponsored by the North American Mixing Forum

WILEY

CHAPTER 3b

Microstructure, Rheology, and Processing of Complex Fluids

PATRICK T. SPICER
UNSW Australia

JAMES F. GILCHRIST
Lehigh University

3b-1 INTRODUCTION

Complex fluids are central to numerous materials and industries, including pulp and paper processing (Bennington, 2004), foods (Schurtenberger, 2004; Fischer and Windhab, 2010), paints (Tadros, 1992), consumer products (Hill, 2004), pesticides and herbicides (Rodham, 2000), and fermentation broths (Nienow, 1998). Complex fluids may be generally defined as fluids containing sufficient polymers, colloids (small particles), droplets, and/or surfactants to affect the fluid's bulk behavior, even at relatively low concentrations. More formally, a complex fluid must have a mesoscopic microstructure, meaning a characteristic length scale between the molecular and macroscopic, which determines its bulk properties (Gelbart and Ben-Shaul, 1996). Figure 3b-1 is an overview of the length scales and contributors to complex fluid structures and rheology where the mesoscopic region is shown over the decades between millimeters and nanometers. A key point is that the characteristic length scale of most complex fluid microstructures is much larger than molecular length scales. As a result, the diffusional relaxation and homogenization time scales for molecular solutions will be far too short to describe complex microstructure fluids. While many mixing processes deal only with the homogeneity of molecular species, microstructured fluids and their larger scale homogeneities are increasingly relevant to industrial mixing.

Advances in Industrial Mixing: A Companion to the Handbook of Industrial Mixing,
First Edition. Edited by Suzanne M. Kresta, Arthur W. Etchells III, David S. Dickey and Victor A. Atiemo-Obeng.

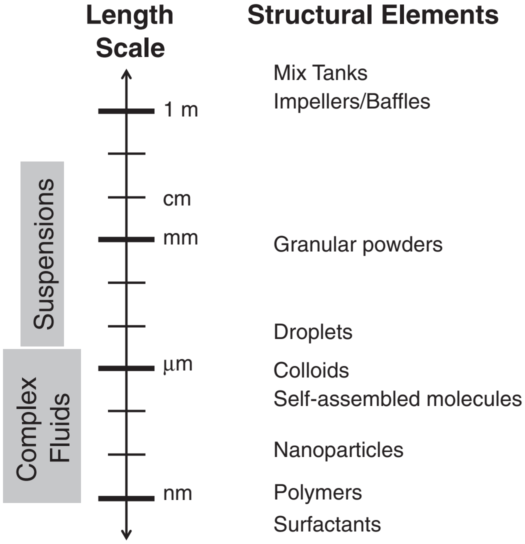

Figure 3b-1 Microstructural elements of non-Newtonian complex fluids, their length scales, and associated process parameters.

Processing is often complicated by the fact that complex fluid rheology can change significantly during mixing-induced microstructural rearrangements. Its not hard to see why knowledge of a fluids rheology is critical to designing a mixing process: The resistance to flow must be directly offset by the mixing energy input. But why should we care about microstructure as much as rheology? One reason is common specification of a process objective as a specific micostructural characteristic, like a particle size, an emulsion droplet size, or a clear solution. However, even without such a constraint, knowledge of the microstructure controlling rheology allows us to understand, and sometimes predict, how rheology will change as a result of mixing and other processes. Mixing complex fluids thus requires an understanding of various rheological measurements, an ability to link such results to an expected microstructure, and awareness of how flow can modify all of the above. Figure 3b-2 encapsulates the motivations and interactions to be considered during complex fluid design, mixing, and application.

This chapter draws on the existing mixing literature to summarize the origins of complex fluid rheological behavior and the characterization, mixing, and applications of such fluids. We begin with an overview of the literature on complex fluid mixing and contrast it with the rheological and complex fluid literature to identify new connections that might provide benefit. An overview of some of the main classes of complex fluids, the types of materials that exhibit such behavior, and their rheology is then given. Building on the rheology section is a section on the use of microrheology to link microstructure and rheology measurements with discussion of its potential

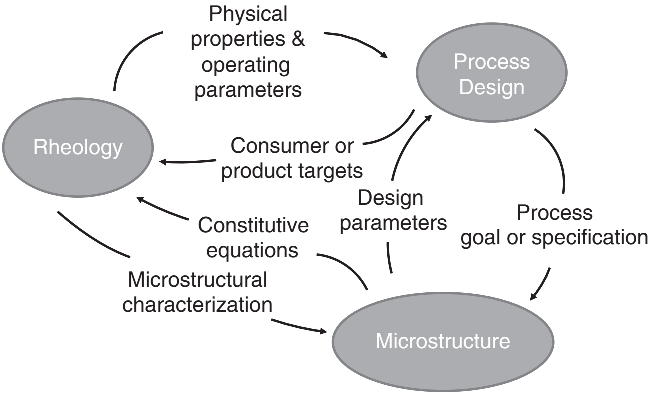

Figure 3b-2 Visualization of the multiple dependencies of complex fluid structure and rheology as well as the ways they can influence, and be influenced by, the process.

to enable characterization of mixing at unusually small length scales. Finally, some examples are provided to demonstrate the current state of complex fluid processing knowledge and to identify and motivate future studies at the boundary between fundamental and applied aspects of this fascinating field. As this chapter focuses on fluid mixing concepts, we point the reader to further reading on complex fluid microstructure (Stokes and Evans, 1997; Larson, 1999; Witten and Pincus, 2010) and rheology (Bird et al., 1987; Baird and Collias, 1998; Larson, 1999) for additional enquiries. Specific fields like food technology have done significant work on mixing of complex fluids (Cullen et al., 2000; Fischer and Windhab, 2010) that will not be dealt with here in any depth but can be found in Chapter 27.

Knowledge of fluid microstructure provides a way to anticipate changes in a fluid's rheology during processing, how those changes affect mixing, and any resulting impacts on product quality. Most discussions of fluid rheology take a continuum approach and assume complete fluid structural homogeneity, and indeed most rheological measurements require such a criterion for accuracy. However, complex fluids can defy such an assumption with highly counterintuitive behaviors. Fluids with heterogeneous structures larger than a micron, or with heterogeneities that form as a result of flow, can often not be treated as fully homogeneous and their rheology and structure can be history- and position-dependent. As a result, not all fluids with the same initial rheology have the same structural or flow response to stress and deformation. Some of the most common questions a mixing practitioner can ask of a rheologist: What value should be used in a given correlation? and When can the rheology be approximated as constant with time or flow? and How will a material property vary with time or stress? will be treated here in the context of understanding the microstructure that drives complex rheological behavior. In this chapter we focus on the case, analogous to reacting systems, when microstructural changes occur more slowly than mixing.

Figure 3b-3 Tag cloud representation of the most frequently used words in over 1000 mixing articles from 1955–2010.

3b-2 LITERATURE ANALYSIS—MIXING OF COMPLEX FLUIDS

So, what is the focus of most mixing studies? Figure 3b-3 shows a tag cloud representation produced by Wordle.net of the titles of 1075 publications from a range of academic and industrial authors. The size of the word indicates its relative frequency of use in the article titles. Immediately obvious is the applied nature of the mixing literature: Words like performance, vessel, impeller, agitated, and flows all appear frequently. The types of fluids studied are also clear: dispersions, polymers, and gas are all visible.

Newtonian fluids and suspensions are prevalent while non-Newtonian fluids like yield stress and shear thinning fluids appear but are smaller because the other topics are more frequently the publication focus. Though qualitative as a survey, the visualization is helpful to remind us that fluid rheology is often viewed more as a fixed physical property than one with as much potential for change as the mixing process itself. It is useful to tunnel down a little more and map the degree of study of complex fluids in mixing contexts.

So what aspects of complex fluid mixing are studied most? The answers to such a question tell us many things: the biggest manufacturing needs, the most interesting research problems, and the best-funded areas, to name just a few. There is, of course, a large body of literature on complex fluid properties themselves and it is also useful to contrast the relative amount of activity for each type of fluid.

Two different approaches are used here. First, a naive Google Scholar search for documents with both mixing and some fluid type classifier in the title was performed and the number of unique documents found was then tallied. The numbers of documents found in each search are plotted in Figure 3b-4. Again, shear thinning is a dominant area of focus although the more general term of viscoelasticity is used most frequently.

A second search for unique documents with just the fluid type in the title was also performed to assess the overall level of scrutiny of a given rheology by any researchers.

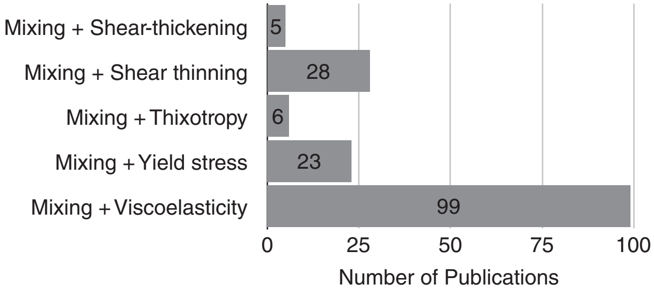

Figure 3b-4 Google Scholar search results for mixing studies of different fluid rheology types.

Figure 3b-5 can then be thought of as a rough measure of the relative activity on a given rheological topic. Interestingly, the dominant fluid types are different than for mixing studies alone. Although viscoelasticity is again dominant here, its generality makes that less of a surprise. The overwhelming imbalance between shear-thinning and yield stress, however, is clear and interesting given that all yield stress fluids are shear-thinning. This indicates the actual yield stress phenomenon itself is still a very active research area that is difficult to model, while shear-thinning behavior is more easily modeled in some contexts. The magnitude of publications is quite different between Figures 3b-4 and 3b-5, so much so that even the least-studied rheology type, shear-thickening, still has more than one hundred times the mixing-focused publications.

Without oversimplifying too greatly, one clear message from such analyses of the literature is that there is much known about the rheology of complex fluids and that there are likely some excellent opportunities to supplement what we know about mixing these fluids by drawing on other fields. It will thus be useful to examine different classes of rheology, the materials and structures that impart such flow behavior, and what we know about their mixing effects.

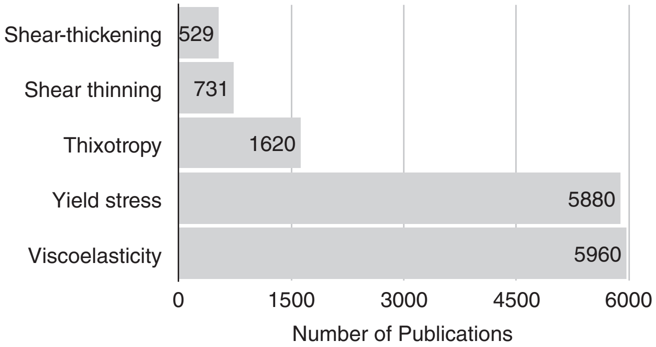

Figure 3b-5 Google Scholar search results for individual studies of complex fluid rheology.

3b-3 COMMON COMPLEX FLUID RHEOLOGY CLASSES AND THEIR EFFECTS

The first exposure to fluid rheology is usually through the concept of viscosity μ, defined as the ratio of shear stress, σ, exerted on or by a fluid to its shear rate, $\dot{\gamma}$:

$$\mu = \frac{\sigma}{\dot{\gamma}} \tag{3b-1}$$

Figure 3b-6 contrasts the basic flow behavior of important complex fluids and provides an excellent starting point for discussion of the additional complexities of flow that can be encountered. The curves in Figure 3b-6 are calculated using limiting values of the Herschel–Bulkley equation:

$$\sigma = \sigma_y + K\dot{\gamma}^n \tag{3b-2}$$

where σ_y is the fluid yield stress, K is a proportionality constant, and n is a power law exponent. Equation (3b-2) is able to describe power-law behavior and includes an additional yield stress term. Shear-thinning fluids have an exponent of $n < 1$, Newtonian fluids are defined by an $n = 1$, and shear-thickening fluids $n > 1$ and on a log-log plot like Figure 3b-6 the n value determines the slope of the flow curve. Yield stress fluids are typically shear-thinning and will not flow until a threshold stress,

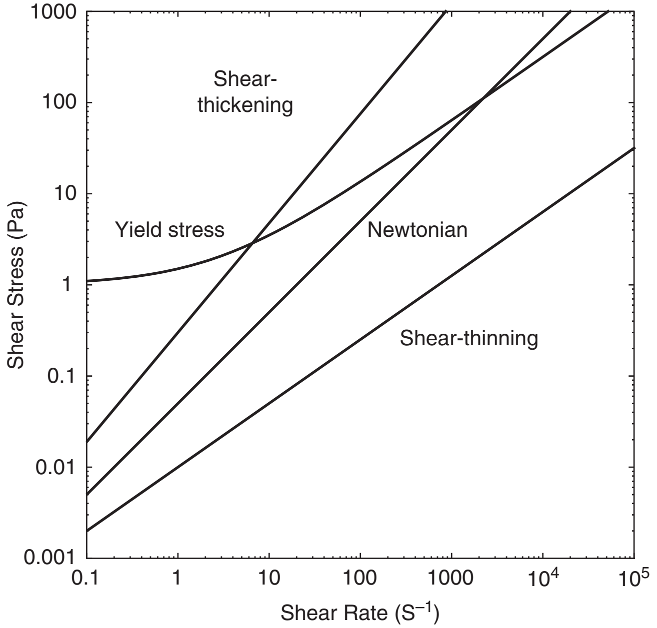

Figure 3b-6 Log-log plots of calculated flow curves for a range of non-Newtonian fluids.

σ_y, is exceeded and in Figure 3b-6 the $\sigma_y = 1$ Pa. Equation (3b-2) can be used to describe important elements of flow for some of the key fluid types encountered in industrial mixing studies but does not provide a complete description. The sections below supplement Figure 3b-6's summary by highlighting additional industrially relevant complex fluid properties and their microstructural origins.

3b-3.1 Shear-Thinning Fluids

Shear-thinning fluids exhibit decreased viscosity with increasing applied shear stresses, by definition. Shear-thinning fluids commonly studied in a mixing context include carboxymethyl cellulose (Elson et al., 1982) and numerous other non-crosslinked polymer solutions and dispersions. Almost all non-Newtonian fluids are shear thinning (Macosko, 1994), but because they represent such a broad class of materials it is useful to map them a bit more so it is clear what fluids can exhibit such behavior and the limits of shear-thinning behavior. For example, all yield stress fluids are shear-thinning but not all shear-thinning fluids have a yield stress.

Figure 3b-7 shows an example of shear-thinning flow by a suspension of spheres. At low shear stress, viscosity is constant. Above a shear stress of 10 Pa, the suspension viscosity decreases by several orders of magnitude as the particles flow past one another more readily. Although not an unusual result, the data in Figure 3b-7 deviate

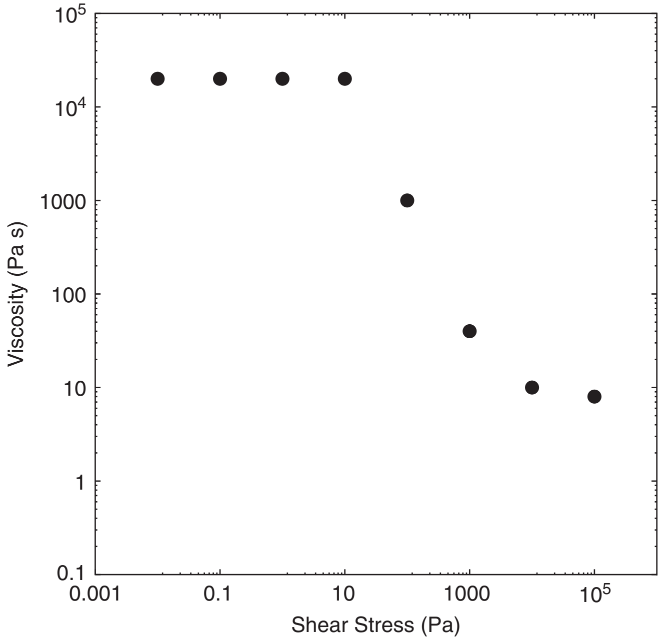

Figure 3b-7 Measured flow curves for a shear-thinning suspension of 60% w/w non-interacting hard spheres (replotted from Mackley and Hassell, 2011).

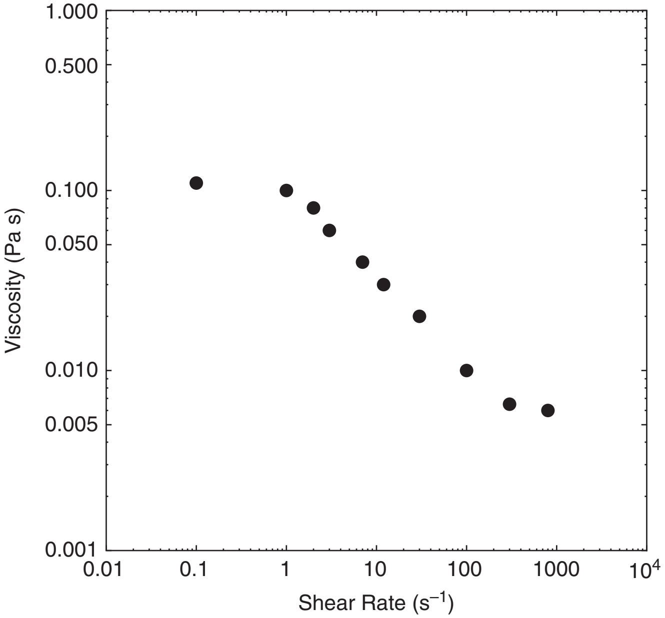

Figure 3b-8 Flow curve for 1000 ppm xanthan gum in water (replotted from Whitcomb and Macosko, 1978).

from the calculated behavior of a power-law fluid because eq. (3b-2) does not predict the viscosity plateau observed at low shear stresses and only accounts for the intermediate thinning flow regime. Such a disagreement is useful to highlight the strength of simple equations or fitted models as well as the need to always consider their limits.

Similar to the above example for a suspension, Figure 3b-8 shows the behavior of a shear-thinning solution of xanthan gum polymer. Just as we can picture the particles sliding past one another after sufficient shear stress has been applied in Figure 3b-7, in Figure 3b-8 we imagine entangled polymer molecules beginning to disentangle and flow. However, it is also appropriate to consider the flow of such a system when there are more complex interactions between the microstructural constituents.

Figure 3b-9 shows the flow of a high concentration of nonionic surfactant that forms a lamellar liquid crystalline phase. While such structures are complex self-assembled structures, their shear-thinning behavior is quite similar to the colloidal and polymeric examples shown earlier. However, liquid crystalline flow behavior is often highly rate-dependent because their large-scale structures can re-orient to form smaller-scale domains such as vesicles. Here different shear histories can determine the flow curve measured and it is critical to establish a baseline flow history for any sample that is a reproducible reference frame against which we can judge different processing effects.

Solutions of micelles, especially those with a rodlike or wormlike character, are an excellent example of a fluid that is well-studied in the rheology and interfacial literature (Schubert et al., 2004) but less so in a mixing context. Much like an

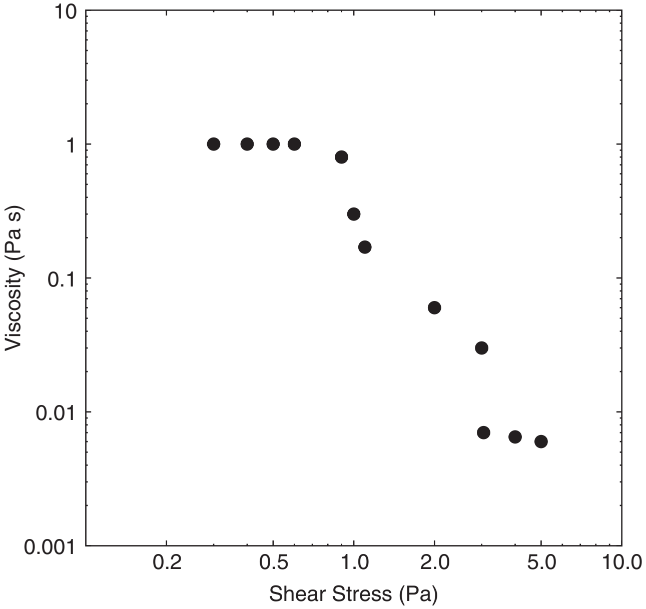

Figure 3b-9 Viscosity with shear rate for SDS[1]-decanol-dodecane-water system in the lamellar liquid crystalline phase exhibiting a Newtonian plateau followed by two different slopes of shear thinning and then a second, lower, plateau (replotted from Roux et al., 1993).

idealized polymer solution, worms are shear-thinning because they flow and entangle one another but simply relax on time scales dictated by their disentangling and breakage/reformation kinetics (Cates and Candau, 1990). Unlike micelles, actual polymer chains in a melt or solution do not break and reform but will similarly flow and entangle, also shear-thinning. Micellar systems represent a potentially new model fluid for mixing studies because of their transparency. Although more complex than Newtonian fluids, shear-thinning fluids are able to flow at even low stresses. In contrast, when shear-thinning fluids develop cross-links between particle, micelle, or polymer structural constituents, a network is created that can resist flow at low stresses and a yield stress fluid is formed.

3b-3.2 Yield Stress Fluids

Yield stress fluids are a solid-like material that doesn't flow until a critical stress is exceeded, after which it flows like a liquid. Modeling such behavior often begins with a non-zero value of the yield stress term in eq. (3b-2).

The expectation that a fluid might have a yield stress comes from an understanding of the fluid microstructure and its relevant length and time scales. Attractive interactions between colloids, physical crowding of larger particles like pulp fibers, and

---

[1] SDS (sodium dodecyl sulfate) is a common surfactant.

cross-links between polymers or micelles can all provide a finite yield stress to a fluid. Concentration is also a key variable in yield stress fluids. Very dilute suspensions can have a yield stress but only if the particles attract each other strongly such that they stick together upon collision. The aggregated structure formed by attractive particles is termed a "gel" if you are a physicist and a "flocculated network" if you are an engineer. Very concentrated granular pulp fiber dispersions can have a yield stress without any appreciable attractive interactions at the fiber level, simply because of physical crowding effects, and such highly concentrated but non-attractive particle suspensions are often referred to as glasses in the physics and colloid literature (Trappe and Sandkuhler, 2004). Cement is an extreme but economically relevant example of a yield stress fluid that has been highly studied in recent years (Jarny et al., 2005), and foods such as mayonnaise and ketchup are popular edible examples.

The rheology of a suspension gel is highly dependent on whether the particles attract one another strongly enough to form a network that resists flow. An example of the yield stress behavior exhibited by a dispersion of flocculated latex particles is seen in Figure 3b-10. There the viscosity diverges rapidly at low stresses but above the yield stress around 1 N/m^2 the suspension is shear-thinning. Gel microstructure is often a unique function of its processing history because the particle networks can grow, break, and re-form under flow so any model of their rheology must include descriptions of the microstructure (Potanin, 1992).

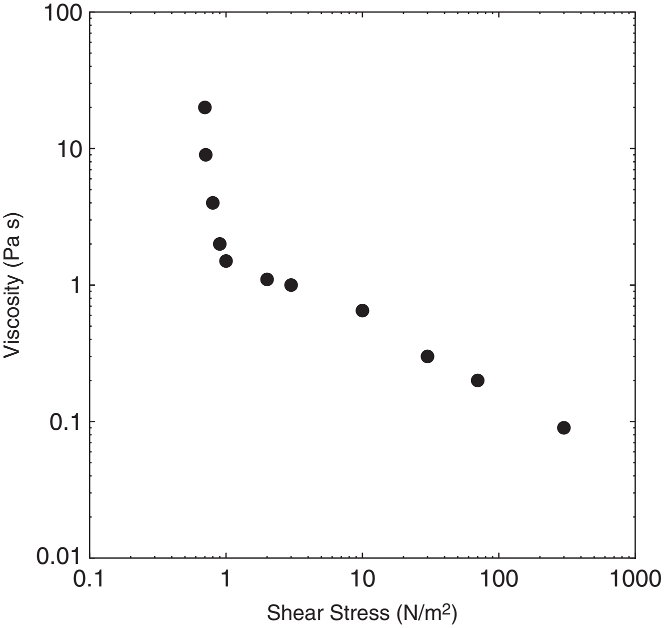

Figure 3b-10 Viscosity over a range of stresses for a dispersion of polystyrene latex showing both shear thinning and yield stress behavior (replotted from Patel and Russel, 1988). At low stress the suspension diverges in viscosity as a result of the attractive interactions induced by added 2.5% w/w dextran polymer.

Besides the considerations of the interactions and concentration of the microstructural constituents of a yield stress fluid, the shape of the particles creating the yield network is also important. The aspect ratio of dispersed particles can play a huge role in setting the yield stress in a fluid when all other conditions are constant. For example, raising the aspect ratio of a network's primary particles can increase the yield stress by orders of magnitude for a given concentration, while higher aspect ratio particles can create a yield stress in a fluid well below the point of spherical close packing (Solomon and Spicer, 2010).

Just as particle suspensions can develop yield stresses as a result of either particle crowding at high concentrations or aggregated networks at low concentrations, so too can polymer solutions with chemical cross-links joining their polymer chains exhibit significant yield stresses (Caggioni et al., 2007). Concentrated surfactant solutions that form highly interconnected liquid crystalline structures can have large yield stresses and take quite long times to relax after yielding in flow (Mezzenga, 2005).

3b-3.2.1 Cavern Formation by Yield Stress Fluids A consequence of mixing yield stress fluids, at least for most situations when fluid flow is not uniform, is that the minimum shear stress in a vessel is often lower than the fluid yield stress. As a result, the system will behave as a solid in regions where yield stress exceeds shear stress and behave as a fluid where yield stress is exceeded by shear stress. One practical form such flows can assume is a cavern, a region of relatively well-mixed fluid in the highest shear stress regions, around an impeller, for example (HIM Volume 1, p. 522). The location of the cavern boundary for a specific system can be mapped by flow visualization using careful dye placement inside the cavern area (Jaworski et al., 1994) and tomography measurements (Bhole et al., 2011) or can be estimated based on stress values calculated radially outward from the impeller zone (Amanullah et al., 1998). Several variations are possible, as shown in Figure 3b-11 for the case of mixed tanks with a central impeller. The most basic cavern type is a band around the impeller, Figure 3b-11*a*, when sufficient shear stress locally yields

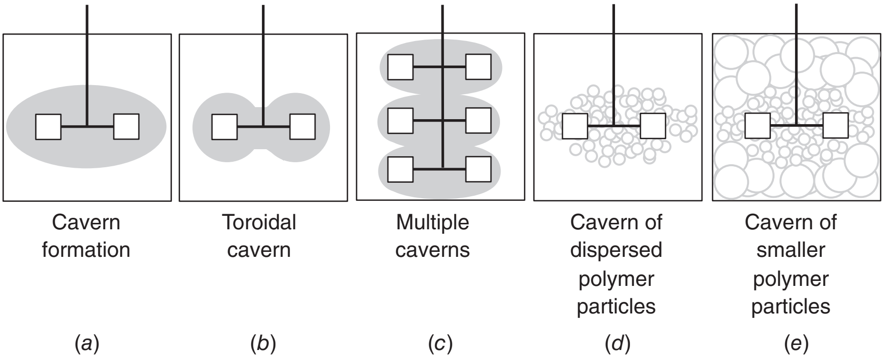

Figure 3b-11 Schematic of different cavern types observed in mixed tanks, where gray areas indicate regions that have mixed and white indicates unmixed areas.

the fluid. More accurately depicted caverns are toroidal regions as in Figure 3b-11*b* (Amanullah et al., 1998). One way of dealing with cavern formation is to employ multiple impellers, as in Figure 3b-11*c*. Although the bulk of the tank is well-mixed by such arrangements, axial distribution can still be limited and the impeller shaft needs to be placed off-center to both yield the fluid and provide axial mixing (Arratia et al., 2006). The examples given in Figures 3b-11*a–c* are idealized in that they assume a continuum fluid without significant history and are used to describe mixing of soluble species on molecular length scales. However, when a fluid has structure on larger length scales, or is cross-linked at the molecular level, additional situations can occur. An example is the formation of a biopolymer gel, e.g., the cooling of a gellan or xanthan gum system. In such cases, the history of the gel is critical to its mixing response and resulting microstructure. If a gelled system is formed under quiescent conditions and then mixed, the situation seen in Figure 3b-11*d* can occur, where the local high shear stresses around the impeller shred the gel into smaller pieces that flow and remain around the impeller region. If the system is instead mixed as it gels the case shown in Figure 3b-11*e* may prevail, where the fluid is dispersed into a distribution of gel fragments with a predominance of smaller pieces centered around the impeller region. Caggioni et al. (2007) examined such history dependence for gellan gum systems and found that particulate ingredients added after dispersion of the gel are located exclusively in the interstitial spaces between gel fragments while particles introduced prior to gelation reside entirely within the gel fragments. Another mixing effect in yield stress fluids is the sometimes stark radial segregation of particles with different size or density as their inertia allows them to move away from their smaller or less dense counterparts (Madani et al., 2009). The discontinuous behavior of yield stress fluids at small length scales can have negative and positive impacts on process efficiency, as the following two example calculations demonstrate.

3b-3.2.2 Example Calculation: Residual Tank Coating after Drainage of Yield Stress Fluid

The shear stress in a fluid draining from a tank decreases rapidly away from the wall, meaning a film of fluid will be retained with a thickness determined by the point where shear stress exceeds yield stress. For a surface with an angle from the horizontal, θ, this critical distance from the wall is given by (Coussot, 2005)

$$h = \frac{\sigma_y}{\rho_l g \sin\theta} \tag{3b-3}$$

For a fluid with a yield stress of $\sigma_y = 10$ Pa and a density of $\rho_l = 1200\ \text{kg/m}^3$, the thickness of the film retained on the vertical wall, ($\sin 90° = 1$), of a tank can be estimated as

$$h = \frac{(10\,\text{Pa})}{(1200\,\text{kg/m}^3)(9.8\,\text{m/s}^2)} = 0.85\,\text{mm} \tag{3b-4}$$

A smaller slope will increase the retention by reducing the gravitational stress contribution. Though the example above yields a small film thickness, such a coating on the entire surface of a large-scale vessel can reduce recovery and complicate cleaning. For example the volume retained on the sides of a cylindrical vessel is

$$V = \pi H \left[\left(\frac{T}{2} \right)^2 - \left(\frac{T}{2} - h \right)^2 \right] \tag{3b-5}$$

so for the case of a 2 meter diameter cylindrical tank with equal liquid height and diameter, H = T:

$$V = \pi\,(2\,\mathrm{m}) \left[\left(\frac{2\,\mathrm{m}}{2} \right)^2 - \left(\frac{2\,\mathrm{m}}{2} - 0.00085\,\mathrm{m} \right)^2 \right] = 0.011\,\mathrm{m}^3 \tag{3b-6}$$

or about 0.17% of the tank volume.

3b-3.2.3 Example: Yield Stress Suspension of Particles A practical aspect of yield stress fluids is their ability to suspend particles in a static fluid without any displacement occurring until some shear stress is applied. It is often useful to estimate the magnitude of yield stress required to suspend a given particle, for example to create a fluid with stably suspended droplets, as in an emulsion product. It is important to contrast this treatment with the Stokes law description of a particle settling in a Newtonian fluid, derived via a force balance between the buoyant and drag forces acting on a suspended particle (Denn, 1980):

$$v = \frac{(\rho_p - \rho_l)d^2 g}{18\mu} \tag{3b-7}$$

where the sedimentation velocity at low Reynolds numbers, v, is a function of the particle, ρ_p, and liquid, ρ_l, densities, the particle diameter, d, gravitational acceleration, g, and the fluid viscosity, μ.

An example of a fluid design needed to stably suspend a particular particle application is a consumer product such as shampoo. We can use eq. (3b-7) to calculate the viscosity required of a Newtonian fluid to suspend a 20 μm diameter spherical silica particle with a density of 2.65 g/cm^3 in a bottle with height h = 20 cm for a product shelf life of t = 1 year. Rearranging eq. (3b-7) to solve for viscosity and substituting the height to shelf life ratio for velocity, we obtain

$$\mu = \frac{(\rho_p - \rho_l)d^2 g t}{18h} \tag{3b-8}$$

and substituting in for the variables above we calculate

$$\mu = \frac{(2.65\,\mathrm{g/cm^3} - 1\,\mathrm{g/cm^3})(0.002\,\mathrm{cm})^2(980\,\mathrm{cm/s^2})(31 \times 10^6\,\mathrm{s})}{(18)(20\,\mathrm{cm})} = 55.7\,\mathrm{Pa\,s} \tag{3b-9}$$

which is more than 500 times the typical value of shampoo viscosity!

We can now contrast the performance of viscosity with that of a yield stress for the same application. A fluid with a yield stress not exceeded by the gravitational stress of a particle is not described by eq. (3b-7) because it essentially possesses an infinite viscosity at low stresses: No flow can occur. By taking the ratio of the particle gravitational stress with the fluid yield stress, and assuming a hemispherical characteristic area of the yield surface formed (Beris et al., 1985), we obtain a dimensionless parameter, Y, that can be used to calculate whether a particle will sediment in a yield stress fluid:

$$Y = \frac{2\pi a^2 \sigma_y}{\frac{4}{3}\pi a^3(\rho_p - \rho_l)g} = \frac{1.5\sigma_y}{a(\rho_p - \rho_l)g} \tag{3b-10}$$

where a is the particle radius and σ_y is the fluid yield stress. It is worthwhile noting that the critical Y, Y_{crit}, bounding the states of suspension and sedimentation, is less than unity because of the finite fluid volume yielded by the particle. This means that the yield stress required to just suspend a given particle is actually less than the gravitational stress the particle exerts. Simulations give a value of $Y_{crit} = 0.14$ (Beris et al., 1985), while experiments produce Y_{crit} values between 0.1 and 0.6 (Chhabra, 2007). Because the critical criterion can vary significantly, so too can the suspension efficiency of a yield stress fluid.

We can use eq. (3b-10) to estimate the yield stress required to stably suspend the above small silica particle by assuming a worst case of a $Y_{crit} = 1$ and use eq. (3b-10) to obtain a yield stress of

$$\sigma_y = \frac{(1)(10 \times 10^{-6}\,\text{m})(1650\,\text{kg/m}^3)(9.8\,\text{m/s}^2)}{1.5} = 0.11\,\text{Pa} \tag{3b-11}$$

which is quite low and would not make the shampoo too viscous to use. So we see that a yield stress can be a very efficient means of stabilizing particle suspensions because it can entirely prevent any particle motion, whereas viscosity merely slows particle motion.

Ultimately eq. (3b-10) is useful as a non-dimensional index if determined for a specific fluid–particle system using an experiment like the one in Figure 3b-12. The suspension stability of a range of particle sizes and/or densities is recorded for a specified yield stress fluid and the transition from stability to sedimentation recorded.

We note that the approach described above applies to sedimentation of a dilute suspension of particles through a homogeneous yield stress fluid or, equivalently, of a much larger single particle through a homogeneous suspension of small particles. In many cases a yield stress is imparted to a fluid by a very concentrated dispersion of non-interacting particles, or by a more dilute dispersion of interacting particles, and the sedimentation of the suspension's particulate structural elements is not described by eq. (3b-11). Sedimentation of entire concentrated particle dispersions is better quantified using hindered settling concepts (Landman and White, 1992), while the collapse of a more dilute colloidal gel is still an active research area (Manley et al., 2005). Just as yield stress fluids can be induced to suddenly flow above a certain stress threshold, shear-thickening fluids are another fascinating non-Newtonian system that suddenly increases in viscosity as a result of flow-induced structural changes.

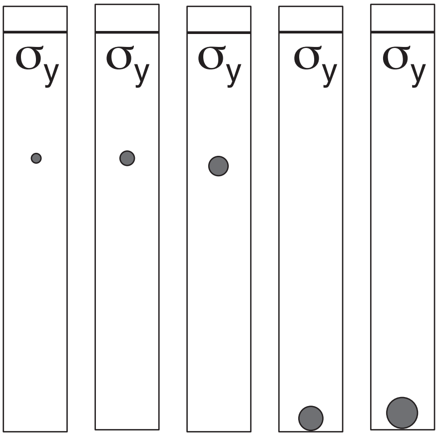

Figure 3b-12 Experiment to determine threshold load of a yield stress fluid.

3b-3.3 Shear-Thickening Fluids

When a fluid increases its viscosity in response to an applied stress it is termed shear thickening. Concentrated suspensions of particles are the most commonly studied form of shear-thickening fluid, where the stress response is thought to occur as short-lived hydroclusters form in the fluid shown in Figure 3b-13 and resist flow (Wagner and Brady, 2009). The hydrocluster structure is not the same as an aggregated cluster because it forms as a result of stress distribution through several contiguous particles and not through attractive adhesion. Figure 3b-14 shows an example of a 60% w/w suspension's flow curve displaying the onset of shear-thickening behavior above a stress around 200 Pa. At lower solids levels, only Newtonian or shear-thinning behavior is observed. Shear-thickening dispersions often have a yield stress and, once flow begins, the fluid can shear-thin as the suspended particles organize in the flow but then thicken again above a certain stress threshold as Figure 3b-13 shows in schematic form.

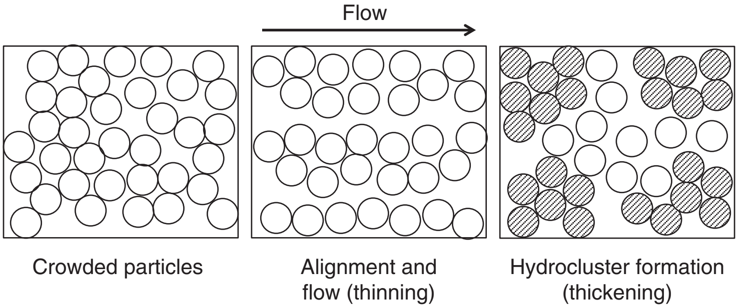

Figure 3b-13 Schematic of the short-lived particle structures formed during suspension flow, thinning, and then thickening (redrawn from Wagner and Brady, 2009).

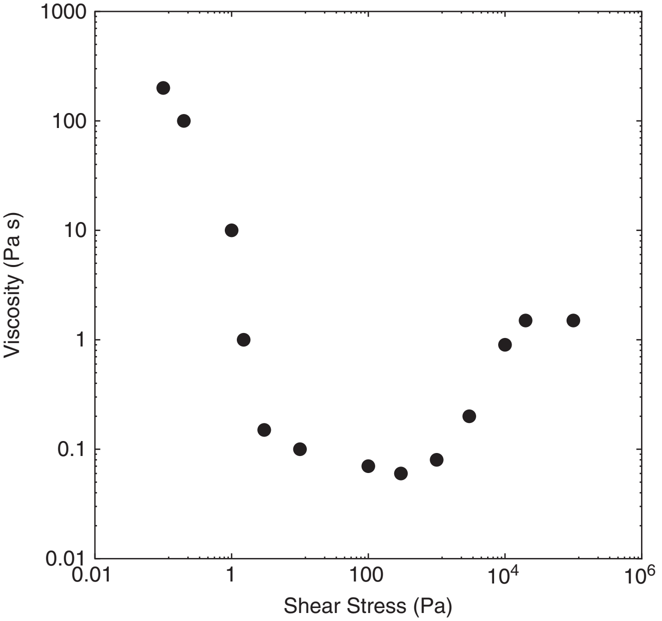

Figure 3b-14 Complex colloidal flow behavior exhibiting shear-thinning, followed by mostly Newtonian flow, then a stark thickening by more than an order of magnitude in viscosity (replotted from Wagner and Brady, 2009).

The mixing of shear-thickening fluids can bring about an effect that is nearly the opposite of cavern formation by yield stress fluids. Delaplace et al. (2000) studied mixing of shear-thickening fluids and found that shear-thickening fluids increase their viscosity to the point of essentially solidifying near the high-energy impeller zone, a sort of inverse cavern. During mixing, local thickening can shift the high shear region away from the impeller toward the wall, requiring calculation of an effective impeller diameter increase (Figure 3b-15) and recognition that baffles can increase power consumption (Delaplace et al., 2000) by a significant factor. In addition to its effects on mixing, shear-thickening liquids can improve the efficiency of high-energy milling processes by better transmitting energy to the milled particles, although thickening can lead to permanent solidification of the fluid if particle bonds are irreversible (Wagner and Brady, 2009). Shear thickening can be used to disperse, for example, hard, agglomerated pigment particles in an approach termed “let down” that also reduces subsequent dispersion viscosity. Shear-thickening fluids have also found fascinating direct application in the creation of stab- and shrapnel-resistant body armor using mineral dispersions layered between strong Kevlar sheets (Egres and Wagner, 2005; Qiao et al., 2008).

Polymeric and surfactant systems can also shear-thicken, though often by different mechanisms. For example, in an extensional flow, polymers that at low deformations only associate with their own coils can be elongated at high deformations so that they

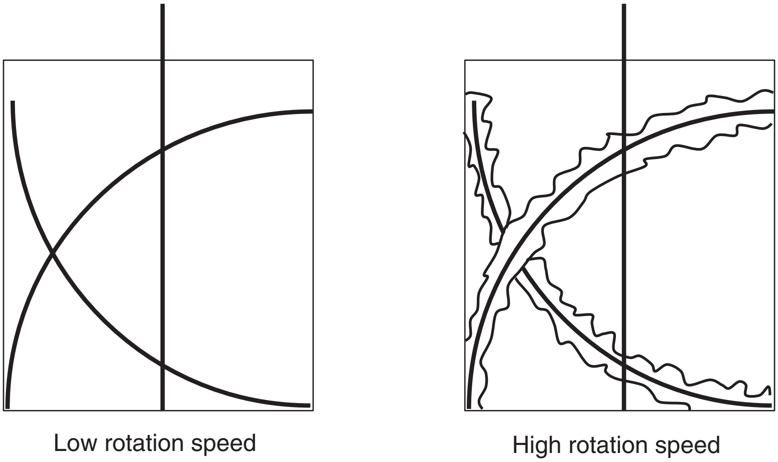

Figure 3b-15 Schematic drawing of the effects of a shear-thickening fluid on the size of a helical impeller. The locally increased viscosity results in an effective increase in the dimensions of the mixer blades, requiring far more energy input than the original equipment (redrawn following Delaplace et al., 2000).

form transient associations with other chains to cause shear-thickening (Ballard et al., 1988). Although studied even less in a mixing context, surfactant-based wormlike micellar systems can also shear-thicken when their concentration is high enough that they briefly jam at high shear rates (Takeda et al., 2011). Unlike very concentrated colloidal dispersions, polymer and surfactant systems that shear-thicken exhibit much smaller magnitudes of viscosity increase, probably because the effect is driven by smaller length scale, and thus faster diffusing, structures below 100 nm versus the micron-scale colloidal systems.

Another effect of fluid relaxation times longer than the time scale of flow is time-dependency or thixotropy, a general term describing the case when fluids flow very differently depending on, for example, whether they experience a high and then low shear rate or a low and then high shear rate, as shown schematically in Figure 3b-16.

3b-3.4 Time-Dependent Fluids

Thixotropy occurs because of a time- and flow-dependent microstructure (Mewis, 1979). More quantitatively, the breakdown and recovery of a thixotropic fluid microstructure, and thus rheology, occurs on time scales similar to, or longer than, the time scales of flow. Fluid properties or additives that slow the structural changes, such as higher viscosity continuous phases or slowly diffusing high aspect ratio dispersed particles, accentuate thixotropy (Mewis, 1979). While simple entanglements can produce thixotropic behavior, microstructural elements with strong attractive interactions can initially exhibit hysteresis but then slowly converge to more reversible

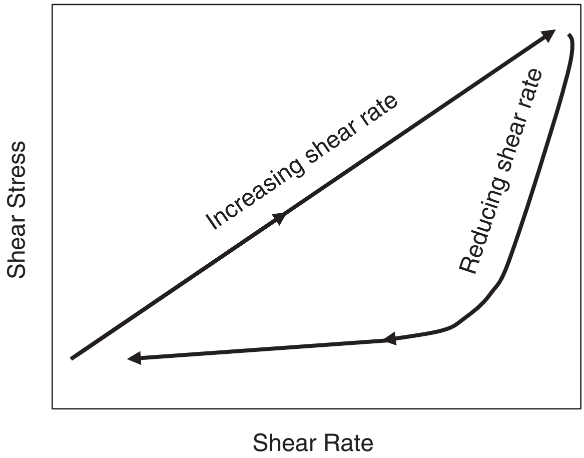

Figure 3b-16 Schematic of hysteretic behavior by a single thixotropic fluid but for rheology measurements made via different directional methods.

behavior. An example is the densification of a flocculated colloidal dispersion following a burst of high energy input: aggregates are broken at their weak points and then re-aggregated at lower energies into denser structures that are nearly impossible to return to their original state (Spicer et al., 1998). Laponite clay dispersions can become increasingly time-dependent by adding small amounts of much smaller particles that interfere with the dispersion's relaxation (Brinke et al., 2007; Ragouilliaux et al., 2007). Thixotropy phenomena are challenging to experimentally characterize because of the uncertainty of uniform flow in many rheometer geometries (Willenbacher, 1996) although NMR experiments are starting to offer more routine flow visualization during flow measurements. One of the most basic yet profound impacts of thixotropy on mixing is likely the history-dependency imparted to the material. For a miscible blending operation time-dependency is often inconsequential, but, when product quality depends on microstructure, it is critical. Some modeling approaches exist that allow the estimation of a material's structural breakdown and reformation kinetics by using its stress response (Dullaert and Mewis, 2006) as an input to aggregation–fragmentation population balance models (Spicer and Pratsinis, 1996).

3b-3.4.1 Suspension Rheology Suspensions of solid particles in a Newtonian fluid are a focus throughout this handbook and the present companion book because of their broad industrial significance and we've shown in this chapter that they can exhibit every major non-Newtonian rheology. Suspensions are a great example of a relatively simple fluid that can exhibit extraordinarily complex rheology because of a strong dominance of microstructure. Understanding spherical particle suspensions with purely hydrodynamic interactions and ignoring electrostatic, particle shape, polydispersity, and non-Newtonian carrier fluid effects is challenging. Though excellent reviews of suspension rheology and flow exist (Guazzelli and

Morris, 2012; Mewis and Wagner, 2011), much of the work has not been connected to industrial mixing. The section below examines both classical and recent suspension work from a mixing perspective.

With the addition of solids to a liquid suspension, the shear viscosity becomes a nonlinear function of solids volume fraction, ϕ. Einstein's early contribution (1906) set the asymptotic dilute limit and Batchelor and Green (1972) contributed a second-order term:

$$\mu_r = \frac{\mu}{\mu_s} = 1 + 2.5\phi + 7.6\phi^2 \tag{3b-12}$$

and emphasized the importance of the proximity of a suspension to close-packing conditions to rheology. At moderate and higher volume fractions, multi-body hydrodynamic interactions quickly matter. For an isotropic fluid with $\phi \sim 0.09$, spherical particles are on average separated by only one particle diameter, and this separation distance decreases sharply with increased solids. Almost no rheological data exist for non-Brownian spheres at $\phi > 0.5$, greatly complicating the description of viscosity divergence as maximum random packing, ϕ_{max}, is approached. A power law dependence is thought to be generally valid in the concentrated regime and Krieger and Dougherty (1959) give

$$\mu_r = \left(1 - \frac{\phi}{\phi_m}\right)^{-2.5\phi_m} \tag{3b-13}$$

where the random close packing volume fraction is $\phi_m = 0.63$. Figure 3b-17 plots eqs. (3b-12) and (3b-13) and shows that viscosity diverges at the jamming limit near ϕ_m. For mixing processes, this divergence causes extreme sensitivity to solids volume fraction for $\phi > 0.25$, especially considering the concentration profile is likely non-uniform in most process conditions.

The viscosity of suspensions depends on microstructure development, and a flow reversal can rupture and reform the microstructure. Experimental data from Gadala-Maria and Acrivos (1980) in Figure 3b-18 show the stress overshoot and undershoot behavior in a suspension. In such cases, there is an initial increase in viscosity, a small decrease, and then an increase to a final steady viscosity as a result of each flow reversal. This represents the initial stress to overcome lubrication forces between neighboring particles, the reduction of viscosity by temporary isotropic arrangement of particles, and the development of a new microstructure leading to the steady stress profile.

3b-3.4.2 *Flow-Induced Phase Separation and Instability* The above sections contrasted fluid microstructure changes and their effects on fluid rheology and mixing but largely focused on cases where the rheological and microstructural description is valid over the entire fluid volume. A more complex form of behavior emerges when collective effects influence rheology and mixing to the extent that instabilities arise. Such behavior is seen in surfactant, polymer, and colloidal systems but since suspension microstructure is readily studied by microscopy, it is often

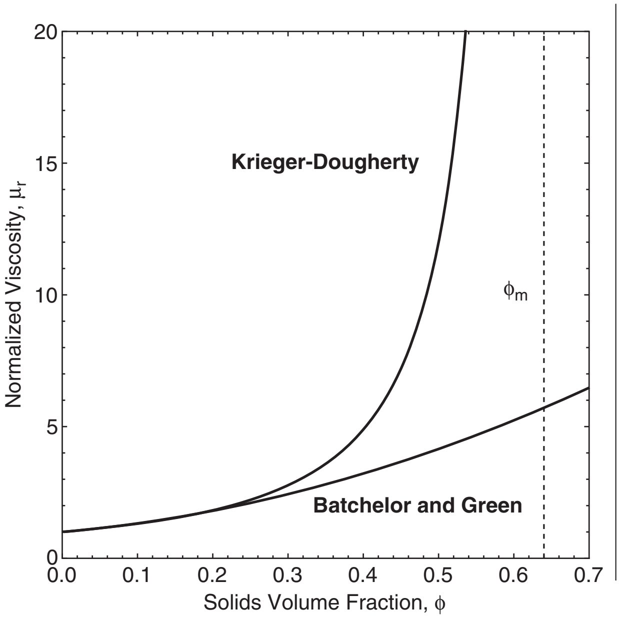

Figure 3b-17 Normalized viscosity, the ratio of suspension viscosity to solvent viscosity, as a function of suspension solids volume fraction.

an excellent analog for complex fluid molecular components such as polymers and surfactants.

An early example of flow-induced instability phenomena was the migration of particles in viscoelastic polymer solution toward flow regions with a zero velocity gradient (Karnis and Mason, 1966). The migration created a depleted area near tube walls with significantly fewer particles (Figure 3b-19). In their system the

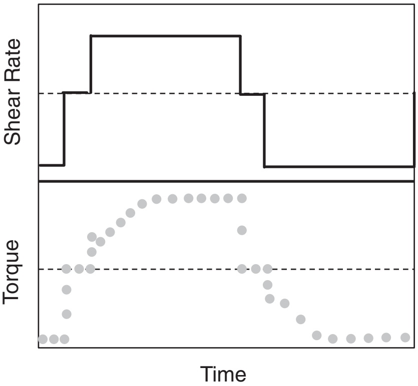

Figure 3b-18 Flow reversal profile showing the effects of microstructure for suspensions (redrawn from Gadala-Maria and Acrivos, 1980).

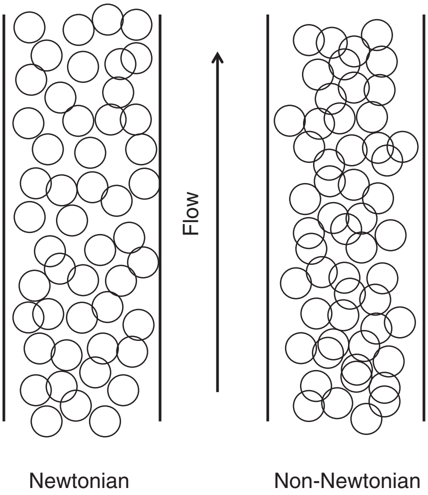

Figure 3b-19 Segregation of suspended particles by normal force gradients in complex fluids.

migration only occurred when the polymer concentration was high enough to create viscoelasticity. They explained the migration as the result of shear rate-dependent normal stresses that apply a net force to the particles until they reach a position of zero shear rate and the normal stresses vanish.

The rate of migration is relatively slow and de-mixing of particles with radius a in a channel of height h scales with $(a/h)^2$, making this phenomenon more significant in microscale flows. In industrially significant flows, shear-enhanced migration has been blamed for demixing near container boundaries and wall-mounted sensors. More recently, Xi and Shapley (2008) used NMR to demonstrate asymmetric bifurcations can effectively filter particles from one stream due to migration. Gilchrist and coworkers have investigated how static microchannel flows optimized to mix Newtonian fluids can fail for suspensions and even enhance the effects of shear-enhanced migration (Gao and Gilchrist, 2008) shown in Figure 3b-20.

Miller et al. (2009) developed a model accounting for the spatial variation of normal stress to describe shear-enhanced migration. For suspensions in expansion and contraction flows, the channel geometry can create a strong directional dependence near corners and cavities, leading to locally higher concentrations. Phillips et al. (1992) developed a diffusive flux model describing migration that includes the local concentration and shear gradient to estimate a cross-streamline particle flux:

$$\frac{D\phi}{Dt} = a^2 K_c \nabla \cdot (\phi^2 \nabla \dot{\gamma} + \phi \dot{\gamma} \nabla \phi) + a^2 K_\eta \nabla \cdot \left(\dot{\gamma} \phi^2 \frac{1}{\mu} \frac{\partial \mu}{\partial \phi} \nabla \phi \right) \tag{3b-14}$$

where $K_c = 0.41$ weights the relative migration related to variations in shear rate and $K_\eta = 0.62$ is for migration related to the local viscosity gradient, with constants estimated from experiments.

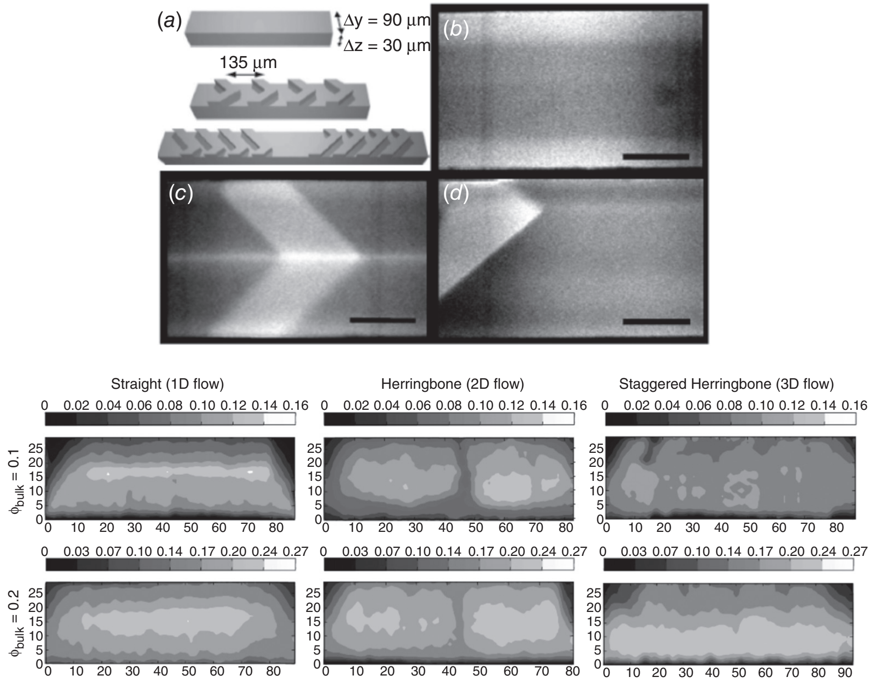

Figure 3b-20 Suspension flow in microchannels showing regions of segregation (reprinted with permission from Gao and Gilchrist, 2008).

Recently, Xu and Gilchrist (2010) used this model to investigate mixing and shear-induced migration in a periodic lid-driven cavity to examine difficulties in mixing suspensions. As shown in Figure 3b-21, in weakly chaotic systems shear migration dominates, while in highly chaotic systems both the convective profile and strength of migration determine the efficiency of mixing and segregation. In this model, it is possible to enhance the effects of migration in a chaotic flow as opposed to the steady lid-driven cavity.

As Figure 3b-19 suggests, segregated flow can be useful for reduction of drag by locally reducing the viscosity of a suspension in large pipes. Such "core-annular flow" can produce a drop in required pumping power by a significant factor and can even be used in liquid–liquid flow when the lower viscosity fluid migrates to the region of highest shear rate and lubricates the more viscous fluid (Joseph et al., 1997).

Throughout this chapter the important interplay of microstructure, rheology, and mixing has been emphasized. Studies of the microstructure have yielded many of the insights cited above, but techniques allowing the study of rheology at the length scale of microstructure are providing complementary information.

3b-3.4.3 Microrheology A central concern of mixing studies is often the determination of homogeneity, so even before the experiment begins a criterion for

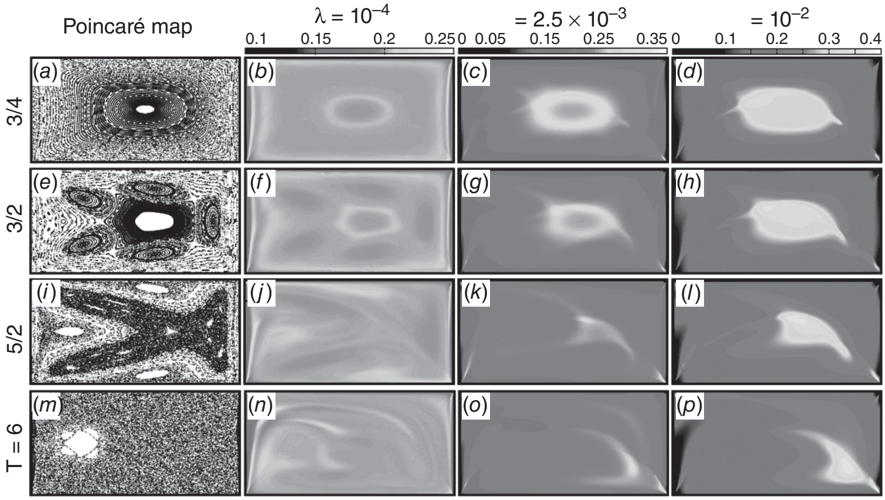

Figure 3b-21 Simulated and experimental flows in cavity (reprinted with permission from Xu and Gilchrist, 2010).

homogeneity or sufficient mixing is necessary. Depending on the application, homogeneity can be required at length scales from the molecular to the millimetric (Figure 3b-1). As in the examples shown above, rheology and microstructure changes can be significant over the same length scale range. Recognizing this fact, researchers developed techniques to systematically measure rheology at increasingly small length scales for a number of reasons: to measure very small fluid volumes, to understand complex fluid flow mechanisms, and to map variations in microstructure that might go undetected by bulk measurements. Microrheology techniques offer an opportunity to simultaneously probe rheology and microstructure at remarkably small length scales and assess mixing in a new way.

Microrheology is primarily a microscopy technique, although scattering methods are also used, where the mobility of a tracer particle is tracked and used to calculate the local rheology of a fluid (Gardel et al., 2005). Two main types of microrheology are used: passive approaches rely on tracer particles small enough to undergo Brownian motion while active methods move tracers using external optical and magnetic forces. In all cases the movement of the particles is related to the surrounding fluid rheology by the statistics of the particle position with time. Basic techniques allow measurement of viscosity, while more advanced methods also provide the viscoelastic properties of a fluid and an assessment of the microstructure homogeneity. Just as the determination of mixing homogeneity requires understanding the proper length scale of scrutiny, the measurement of microrheology requires specification of the relevant length scale being characterized. Figure 3b-22 shows three cases where the length scale of the tracer particle used in a microrheology experiment is varied to extract information about the bulk fluid, the fluid's structural constituents, or the background solvent. Although only a few examples of microrheological mixing studies currently exist

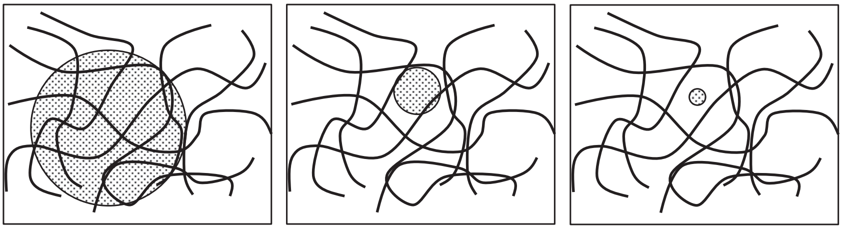

Tracer particle larger than the microstructure: rheology measured is comparable to bulk measures

Tracer particle similar in size to the microstructure: measures mechanical properties of structural elements

Tracer particle much smaller than the microstructure: background fluid rheology is measured

Figure 3b-22 Different cases where microrheology is used to assess fluid properties, defining the length scale of scrutiny in each case.

(Caggioni et al., 2007), more fundamental studies are beginning to offer new insights into familiar mixing phenomena at very small length scales. Choi and Squires (2010) used a 20 μm disk, rotated by a magnetic field, to visualize the equivalent of a tiny yielded cavern at the interface of a complex surfactant solution.

3b-4 CONCLUSIONS

Complex fluid mixing is a topic of broad interest, application, and active research, and this chapter has highlighted elements of each but only hinted at the depth and breadth of the field. Other related areas such as granular solid mixing, pulp dispersion processes, food mixing, microfluidics, and actual scale-up criteria for non-Newtonian systems are dealt with in Chapters 15, 20, 27, 7, and 16, respectively.

Whether engineering a process or a fluid, the interactions between mixing, microstructure, and rheology are strongly coupled. When working with complex fluids, two approaches can be taken. First, a product-focused approach seeks to control microstructure by varying composition and processing history to yield a product that matches the end-user specifications. A process design approach often tries to control fluid flow properties by altering microstructure. In this case, transport of constituents is the first priority and the development of efficient processes to handle these materials must consider the fluids changing rheological properties and its impact on mixing and transport. These two approaches represent product development and process development, and both require knowledge of the effects of rheology on mixing as well as the effects of mixing on rheology.

NOMENCLATURE

a	particle radius
d	particle diameter

g	gravitational acceleration
h	height
H	liquid height
K	constant
K_c	constant
K_η	constant
n	power law exponent
t	time
T	tank diameter
v	velocity
V	volume
Y	dimensionless yield stress

Greek Symbols

μ	viscosity
μ_r	reduced viscosity
μ_s	continuous phase viscosity
$\dot{\gamma}$	shear rate
ϕ	volume fraction
ϕ_m	maximum packing fraction
ρ_l	liquid density
ρ_p	particle density
σ	shear stress
σ_y	yield stress
θ	angle from horizontal

REFERENCES

Amanullah, A., S. Hjorth, and A. Nienow (1998). A new mathematical model to predict cavern diameters in highly shear thinning, power law liquids using axial flow impellers, *Chem. Eng. Sci.*, **53**, 455–469.

Arratia, P., J. Kukura, J. Lacombe, and F. Muzzio (2006). Mixing of shear-thinning fluids with yield stress in stirred tanks, *AIChE J.*, **52**, 2310–2322.

Baird, D. G., and D. I. Collias (1998). *Polymer Processing: Principles and Design*, Wiley, New York.

Ballard, M. J., R. Buscall, and F. A. Waite (1988). The theory of shear-thickening polymer solutions, *Polymer*, **29**, 1287–1293.

Batchelor, G. L., and J. T. Green (1972). The determination of the bulk stress in a suspension of spherical particles to order C^2, *J. Fluid Mech.*, **56**, 401–427.

Bennington, C. P. J. (2004). Mixing in the pulp and paper industry, in E. L. Paul, V. A. Atiemo-Obeng, S. M. Kresta, eds., *Handbook of Industrial Mixing*, Wiley, Hoboken, NJ.

Beris, A., J. Tsamopoulos, R. Armstrong, and R. Brown (1985). Creeping motion of a sphere through a Bingham plastic, *J. Fluid Mech.*, **158**, 219–244.

Bhole, M. R., L. K. Hui, C. Gomez, C. P. J. Bennington, and G. A. Dumont (2011). The effect of off-wall clearance of a side-entering impeller on the mixing of pulp suspensions in a cylindrical stock chest, *Can. J. Chem. Eng.*, **89**, 985–995.

Bird, R., C. F. Curtiss, R. Armstrong, and O. Hassager (1987). *Dynamics of Polymeric Liquids*, Vol. 2: *Kinetic Theory*, Wiley, New York.

Brinke, A., L. Bailey, H. Lekkerkerker, and G. Maitland (2007). Rheology modification in mixed shape colloidal dispersions. Part II: Mixtures, *Soft Matter*, **3**, 1145–1162.

Caggioni, M., P. Spicer, D. Blair, and D. Weitz (2007). Rheology and microrheology of a microstructured fluid: The gellan gum case, *J. Rheol.*, **51**, 851–865.

Cates, M., and S. Candau (1990). Statics and dynamics of wormlike micelles, *J. Phys. Cond. Matt.*, **2**, 6869–6892.

Chhabra, R. P. (2007). *Bubbles, Drops, and Particles in Non-Newtonian Fluids*, CRC Press, Boca Raton, FL.

Choi, H., and T. Squires (2010). Dynamics within surfactant monolayers, *Phys. Fluids*, **22**, 091113.

Coussot, P. (2005). *Rheometry of Pastes, Suspensions, and Granular Materials*, J Wiley, Hoboken, NJ.

Cullen, P. J., A. P. Duffy, and C. P. O'Donnell (2000). Process viscometry for the food industry, *Trends Food Sci. Tech.*, **11**, 451–457.

Delaplace, G., J. Leuliet, and G. Ronse (2000). Power requirement when mixing a shear thickening fluid with a helical ribbon impeller type, *Chem. Eng. Technol.*, **23**, 329–335.

Denn, M. M. (1980). Process fluid mechanics (pp. 67–71). Englewood Cliffs, NJ: Prentice-Hall.

Dullaert, K., and J. Mewis (2006). A structural kinetics model for thixotropy, *J. Non-Newt. Fluid Mech.*, **139**, 21–30.

Egres, R., and N. J. Wagner (2005). The rheology and microstructure of acicular precipitated calcium carbonate colloidal suspensions through the shear thickening transition, *J. Rheol.*, **49**, 719–746.

Einstein, A. (1906). Eine neue Bestimmung der Molekuldimensionen, *Annal. Phys.*, **19**, 289–306.

Elson, T., J. Solomon, A. Nienow, and G. Pace (1982). The interaction of yield stress and viscoelasticity on the Weissenberg effect, *J. Non-Newt. Fluid Mech.*, **11**, 1–22.

Fischer, P., and E. Windhab (2010). Rheology of food materials, *Curr. Opin. Colloid Interf. Sci.*, **16**, 36–40.

Gadala-Maria, F., and A. Acrivos (1980). Shear-induced structure in a concentrated suspension of solid spheres, *J. Rheol.*, **24**, 799.

Gao, C., and J. F. Gilchrist (2008). Shear-induced particle migration in one-, two-, and three-dimensional flows, *Phys. Rev. E*, **77**, 025301.

Gardel, M. L., M. T. Valentine, and D. A. Weitz (2005). Microrheology, in K. Breuer, ed., *Microscale Diagnostic Techniques* (pp. 1–49), Springer Berlin Heidelberg.

Gelbart, W., and A. Ben-Shaul (1996). The new science of complex fluids, *J. Phys.Chem.*, **100**, 13169–13189.

Guazzelli, E., and J. Morris (2012). *A Physical Introduction to Suspension Dynamics*, Oxford.

Hill, M. J. (2004). Product and process design for structured products, *AIChE J.*, **50**, 1656–1661.

Jarny, S., N. Roussel, S. Rodts, F. Bertrand, R. Le Roy, and P. Coussot (2005). Rheological behavior of cement pastes from MRI velocimetry, *Cement Concrete Res.*, **35**, 1873–1881.

Jaworski, Z., A. Pacek, and A. Nienow (1994). On flow close to cavern boundaries in yield stress fluids, *Chem. Eng. Sci.*, **49**, 3321–3324.

Joseph, D. D., R. Bai, K. P. Chen, and Y. Y. Renardy (1997). Core-annular flows, *Ann. Rev. Fluid Mech*, **29**, 65–90.

Karnis, A., and S. G. Mason (1966). Particle motions in sheared suspensions XIX. Viscoelastic media, *J. Rheol.*, **10**, 571.

Krieger, I. M., and T. J. Dougherty (1959). Concentration dependence of the viscosity of suspensions, *Trans. Soc. Rheol.*, **3**, 137.

Landman, K. A., and L. R. White (1992). Determination of the hindered settling factor for flocculated suspensions, *AIChE J.*, **38**, 184–192.

Larson, R. G. (1999). *The Structure and Rheology of Complex Fluids (Topics in Chemical Engineering)*, Oxford University Press, Oxford.

Mackley, M. R., and D. G. Hassell (2011). The multipass rheometer a review, *J. Non-Newt. Fluid Mech.*, **166**, 421–456.

Macosko, C. (1994). *Rheology: Principles, Measurements, and Applications*, Wiley, New York.

Madani, A., S. Storey, J. Olson, I. Frigaard, J. Salmela, and D. Martinez (2009). Fractionation of non-Brownian rod-like particle suspensions in a viscoplastic fluid, *Chem. Eng. Sci.*, **65**, 1762–1772.

Manley, S., J. Skotheim, L. Mahadevan, and D. Weitz (2005). Gravitational collapse of colloidal gels, *Phys. Rev. Lett.*, **94**, 1–4.

Mewis, J. (1979). Thixotropy—A general review, *J. Non-Newt. Fluid Mech.*, **6**, 1–20.

Mewis, J., and N. J. Wagner (2011). *Colloidal Suspension Rheology*. Cambridge University Press, Cambridge.

Mezzenga, R. (2005). Shear rheology of lyotropic liquid crystals: A case study, *Langmuir*, **21**, 3322–3333.

Miller, R. M., J. P. Singh, and J. F. Morris (2009). Suspension flow modeling for general geometries, *Chem. Eng. Sci.*, **64**, 4597.

Nienow, A. (1998). Hydrodynamics of stirred bioreactors, *Appl. Mech. Rev.*, **51**, 3–32.

Patel, P., and W. A. Russel (1988). Mean field theory for the rheology of phase separated or flocculated dispersions, *Colloid Surf.*, **31**, 355–383.

Phillips, R. J., R. J. Armstrong, R. A. Brown, A. L. Graham, and J. R. Abbott (1992). A constitutive equation for concentrated suspensions that accounts for shear-induced particle migration, *Phys. Fluids A*, **4**, 30.

Pisano, G. P. (1997). *The Development Factory: Unlocking the Potential of Process Innovation*, Harvard Business Press, Cambridge.

Potanin, A. (1992). On the model of colloid aggregates and aggregating colloids, *J. Chem. Phys.*, **96**, 9191–9200.

Qiao, P., M. Yang, and F. Bobaru (2008). Impact mechanics and high-energy absorbing materials: review, *J. Aerosp. Eng.*, **21**, 235–248.

Ragouilliaux, A., et al. (2007). Transition from a simple yield-stress fluid to a thixotropic material, *Phys. Rev. E*, **76**, 1–5.

Rodham, D. K. (2000). Colloid and interface science in formulation research for crop protection products, *Curr. Opinion Colloid Interface Sci.*, **5**, 280–287.

Roux, D., F. Nallet, and O. Diat (1993). Rheology of lyotropic lamellar phases, *Europhys. Lett.*, **24**, 53–58.

Schubert, B. A., N. J. Wagner, E. W. Kaler, and S. R. Raghavan (2004). Shear-induced phase separation in solutions of wormlike micelles, *Langmuir*, **20**, 3564–3573.

Schurtenberger, P. (2004). Understanding foods as soft materials, *Nat. Mat.*, **4**, 729–740.

Solomon, M. J., and P. T. Spicer (2010). Microstructural regimes of colloidal rod suspensions, gels, and glasses, *Soft Matter*, **6**, 1391–1400.

Spicer, P. T., and S. E. Pratsinis (1996). Coagulation and fragmentation: Universal steady state particle size distribution, *AICHE J.*, **42**(6), 1612–1620.

Stokes, R. J., and D. F. Evans (1997). *Fundamentals of Interfacial Engineering*, Wiley, New York.

Tadros, T. F. (1992). Control of stability/flocculation and rheology of concentrated suspensions, *Pure Appl. Chem.*, **64**, 1715–1720.

Takeda, M., et al. (2011). Rheo-SANS studies on shear-thickening/thinning in aqueous rodlike micellar solutions, *Langmuir*, **27**, 575–577.

Trappe, V., and P. Sandkuhler (2004). Colloidal gels-low-density disordered solid-like states, *Curr. Opinion Colloid Interface Sci.*, **8**, 494.

Wagner, N. J., and J. F. Brady (2009). Shear thickening in colloidal dispersions, *Phys. Today*, **62**, 27–32.

Whitcomb, P., and C. Macosko (1978). Rheology of xanthan gum, *J. Rheol.*, **22**, 493.

Willenbacher, R. D. (1996). Unusual thixotropic properties of aqueous dispersions of laponite, *J. Colloid Interface Sci.*, **182**, 501–510.

Witten, T. A., and P. A. Pincus (2010). *Structured Fluids*, Oxford University Press, Oxford.

Xi, C., and N. C. Shapley (2008). Flows of concentrated suspensions through an asymmetric bifurcation, *J. Rheol.*, **52**, 625.

Xu, B., and J. F. Gilchrist (2010). Shear migration and chaotic mixing of particle suspensions in a time-periodic lid-driven cavity, *Phys. Fluids*, **22**, 053301.